

Stellar Hydrodynamics in Radiative Regions

Patrick A. Young, Karen A. Knierman, Jane R. Rigby, and David Arnett

Steward Observatory, University of Arizona, 933 N. Cherry Avenue, Tucson AZ 85721

payoung@as.arizona.edu, kknierman@as.arizona.edu, jrigby@as.arizona.edu,
darnett@as.arizona.edu

ABSTRACT

We present an analysis of the response of a radiative region to waves generated by a convective region of the star; this wave treatment of the classical problem of “overshooting” gives extra mixing relative to the treatment traditionally used in stellar evolutionary codes. The interface between convectively stable and unstable regions is dynamic and nonspherical, so that the nonturbulent material is driven into motion, even in the absence of “penetrative overshoot.” These motions may be described by the theory of nonspherical stellar pulsations, and are related to motion measured by helioseismology. Multi-dimensional numerical simulations of convective flow show puzzling features which we explain by this simplified physical model. Gravity waves generated at the interface are dissipated, resulting in slow circulation and mixing seen outside the formal convection zone. The approach may be extended to deal with rotation and composition gradients (“semiconvection”).

Tests of this description in the stellar evolution code TYCHO produce carbon stars on the asymptotic giant branch (AGB), an isochrone age for the Hyades and three young clusters with lithium depletion ages from brown dwarfs, and lithium and beryllium depletion consistent with observations of the Hyades and Pleiades, all without tuning parameters. The potential insight into the different contributions of rotational and hydrodynamic mixing processes could have important implications for realistic simulation of supernovae and other questions in stellar evolution.

Subject headings: stars: evolution - stars: fundamental parameters - hydrodynamics - convection - lithium

1. INTRODUCTION

The nature of mixing in stars is a perpetual problem in stellar evolution. The standard mixing length theory of convection (Kippenhahn & Weigert 1990) is remarkably effective for

a one-dimensional, ensemble average of convective energy transport. However, observations seem to indicate that more mixing occurs in stars than is expected. For example, measurements of the apsidal motion of binary star orbits give a measure of the density structure of the components. Comparisons with mixing-length models indicate that real stars have larger convective cores than predicted by theory (Young, Mamajek, Arnett, & Liebert 2001). Models of double-lined, eclipsing binaries with well determined masses and radii also require additional mixing to match observations (Young, Mamajek, Arnett, & Liebert 2001; Pols et al. 1997; Ribas et al. 2000). Determinations of young cluster ages independent of isochrone fits to the main sequence using the lithium depletion edge in brown dwarfs give substantially older ages which can also be reconciled by increased mixing (Stauffer et al. 1998).

Parameterized descriptions of mixing can tell us a great deal, but only in well populated regions of the H-R diagram where high-quality observational constraints are numerous. Light element depletion on the pre-main sequence (pre-MS) and convective core sizes, and thus lifetimes and luminosities, on the main sequence are affected (Piau & Turck-Chièze 2002; Young, Mamajek, Arnett, & Liebert 2001). For low and intermediate mass stars s-process nucleosynthesis on the AGB, ISM enrichment, and white dwarf sizes and compositions are strongly influenced (Wallerstein & Knapp 1998). In massive stars the size of the heavy element core and mixing in the high-temperature burning shells may substantially impact supernova nucleosynthesis and explosion mechanisms (BA98,AA00).

It has long been known (Spiegel 1972) that mixing-length theory, by approximating derivatives poorly, must have problems at the interface between convective and nonconvective regions, posing an embarrassment for stellar evolution. Saslaw & Schwarzschild (1965) discussed the problem using laminar hydrodynamic theory in the convection zone, which ignores the strongly turbulent nature of stellar convection. Shaviv & Salpeter (1973) examined the ballistics of a convective blob; this particle approach does not impose continuity (mass conservation) on the dynamics. These two approaches are well represented in the extensive literature on the subject. Most modern stellar evolution codes seem to use either mixing length theory (Kippenhahn & Weigert 1990; Clayton 1983) or the full spectrum theory (Canuto & Mazzitelli 1991) in the turbulent regions and assume other regions are static.

We note that the correct equations for describing stellar *nonconvective* regions are hydrodynamic, not static (Cox 1980). If symmetry is broken, as by perturbations from a convective region, these motions are also three-dimensional. We examine the hydrodynamics induced in radiative regions, due to the fact that the convective/nonconvective interface is neither static nor spherical. The problem becomes one of driven, non-radial, non-adiabatic pulsations (Hansen & Kawaler 1994). Numerical simulations (especially Bazàn & Arnett (1998)

BA98, and Asida & Arnett (2000) AA00) lead us to the possibility that large wavelength modes, specifically plumes, are dominant in the coupling at this interface. We suggest how this coupling works, and how it necessarily implies a slow mixing into the radiative region. We show how a simple version of this picture may be implemented in a stellar evolutionary code. Our theory is complementary to theories of the turbulent convective region, such as the standard mixing length theory (Kippenhahn & Weigert 1990) or the full spectrum theory (Canuto & Mazzitelli 1991).

In this paper we focus on the simplest case, and provide a lower limit on “extra” mixing — which is above that obtained with conventional stellar evolution theory. We argue that our theory is a necessary part of a complete solution, but believe that other aspects of hydrodynamics (such as rotation (Maeder & Meynet 1989; Kumar & Quataert 1997; Schatzman 1999; Charbonnel & Talon 1999; Pinsonneault et al. 2002; Talon, Kumar, & Zahn 2002)) are also important, and may be synthesized into a more complete theory. We present several tests of our approach by comparison with observations.

2. Implications of Numerical Simulations

We begin by examining multidimensional numerical simulations, which are nonlocal and fully nonlinear. We have been most influenced by BA98 and AA00, but have also studied Porter et al. (2001) and Brummell, Clune, & Toomre (2002) in some detail. These simulations give us a glimpse of the hydrodynamic behavior of the interface of the convection zone, from which we can begin to construct a theoretical picture. These simulations are not entirely accurate descriptions of the star due to the limited range of resolution. Turbulent structure is expected to span all size scales down to the local diffusion scale, which is much smaller than the resolution element of any simulation which captures the large scale structure. Further impact of sub-resolution scale physics is discussed in Canuto (2000). The maximum Reynolds number of the simulations (in 3D) to $R \sim 10^8$, whereas in stars R may be as high as 10^{14} . Turbulence may become completely chaotic at $R \gg R_0$, a regime which is not amenable to exploration numerically or experimentally (Dimotakis 2001). While microscopic mixing is not well treated because it is dominated by processes with length scales smaller than the resolution of the simulations, energy and bulk transport are dominated by processes with large length scales, and may be modeled better. It is necessary to develop a theoretical understanding of the processes involved, rather than relying entirely upon numerical results.

These simulations presented us with two puzzles:

- Large density perturbations appear at the interface between convective and noncon-

vective regions (BA98).

- Slow vortex motion appears outside the formally convective region, giving a slow mixing (AA00).

How can this be understood?

2.1. Convective forcing

Inside a stellar convection zone, the velocity field has significant vorticity; outside the velocity is assumed negligible. Hydrodynamically, this interface corresponds to a *surface of separation* between rotational ($\nabla \times \mathbf{v} \neq \mathbf{0}$) and irrotational flow ($\nabla \times \mathbf{v} = \mathbf{0}$) (Landau & Lifshitz 1959), see §34.

To be specific we consider the outer edge of a convective oxygen burning shell (BA98,AA00). This is a simple case in that it avoids the added complexity of a photospheric boundary condition (as opposed to simulations of the solar convection zone, for example Christensen-Dalsgaard (2002); Freytag, Ludwig, & Steffan (1996)) and can be evolved numerically on the evolutionary timescale, since the nuclear and sound-travel timescales are commensurate. The convection does work on the interface between laminar and turbulent regions, with a total power (luminosity)

$$L_{conv} = A\delta P v = APv_s(\delta P/P)(v/v_s), \quad (1)$$

where $A = 4\pi r^2$ is the spherical area, v_s is the sound speed, v the transport velocity by convection, and δP the pressure fluctuation. Inserting numerical values from the simulations we find

$$(\delta P/P)(v/v_s) = 10^{-4} \quad (2)$$

and since $(\delta P/P) \simeq (v/v_s)$, we have a Mach number of

$$(v/v_s) = 10^{-2}. \quad (3)$$

This estimate uses mathematical relations in the spirit of mixing length theory, and gives an average velocity. Examination of the numerical results shows that the actual velocity is concentrated in plumes which occupy a smaller cross-sectional area, but have higher speeds (Hurlburt, Toomre, & Massaguer 1996). There are significant density perturbations at the boundary between laminar and turbulent flow. This is sufficient to drive a nontrivial acoustic flux and cause significant non-radial density perturbations $\delta\rho/\rho$ of a few percent (see BA98, figure 3 and figure 7 and AA00, figure 8).

For earlier and less vigorous burning stages, the Mach number is smaller, so that neglect of acoustic flux may not be so atrocious. However, these stages are also longer, so that the accumulated effect of the waves may still be significant. These enhanced density variations at the interface are a robust feature in simulations; three-dimensional calculations of the solar convective zone and red giant stars have displayed similar pumping of gravity waves (Brummell, Clune, & Toomre 2002; Porter et al. 2001).

In the stellar interior, convective luminosity may be estimated without any detailed theory of convection. The hydrodynamic motion is nearly adiabatic, so the radiative flux is close to that for radiative diffusion for an adiabatic temperature gradient. The total luminosity is determined from the conservation of energy, so that the convective luminosity is the difference $L_{conv} = L_{total} - L_{rad}$ (Kippenhahn & Weigert 1990). At the edge of the convective region, we identify this with the energy flux available to drive waves by the deceleration of plumes. The precise fraction of the luminosity that goes into driving depends upon the detailed physics of the convective interface (Goldreich, Murray, & Kumar 1994); our simulations suggest the kinetic part is comparable to the thermal part of the convective flux (BA98, figure 3).

2.2. Hydrodynamic response

What does this do to the radiative region? The natural modes for nearly laminar flow are irrotational, and in general will be incommensurate with the rotational flows of the convective zone. There will be a mismatch at the boundary, so that the boundary matter will be driven, exciting waves. Because the motion of the plumes is generally subsonic, the coupling will be biased toward g-modes, which have longer periods. Asida & Arnett (2000) find a combination of waves, having both g-mode and p-mode character (Cowling 1941). The waves exhibit an exponential fall-off moving away from the interface into the radiative region, but also significant compressible effects (density fluctuations). See AA00, figures 8, 11-14 for detail.

Figure 1 shows a schematic of the behavior of the interface of the convective region. Three dimensional simulations of convection also show up-down asymmetry (Porter et al. 2001; Brummell, Clune, & Toomre 2002). For the solar convective envelope, with driving caused by the entropy decrease from radiative loss near the photosphere, plumes tend to move downward from the photospheric surface. For oxygen shell burning, plumes tend to move upward from the burning shell, in which nuclear energy release causes an entropy increase. Neutrino cooling tends to cause plumes that are directed downward (BA98).

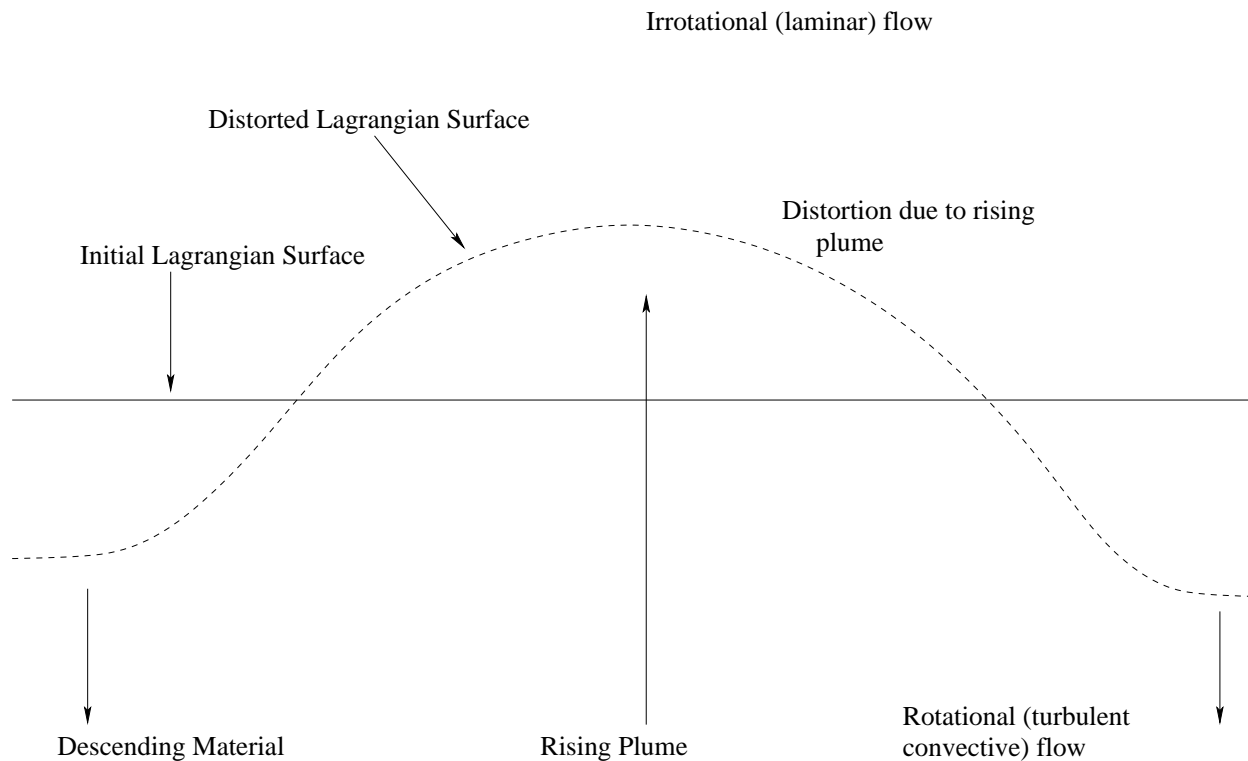


Fig. 1.— Lagrangian (co-moving) fluid surfaces at boundary between convectively stable and unstable regions. The distortion due to a rising plume and a downdraft are shown. The original spherical boundary is distorted as interface material bobs up and down, generating gravity waves. Contrary to the usual assumption in stellar evolution simulations, the convective boundary is neither spherical nor static. Dissipation of the gravity waves actually causes slow circulation in the nominally laminar region outside the convective zone.

As a plume encounters a boundary, it pushes the over(under)lying material, distorting the boundary. Part of the plume’s kinetic energy goes into raising the potential energy of the displaced region. When the plume stalls, this potential energy is converted into motion in the opposite direction of the plume’s velocity. Gravity waves are generated. Contrary to the usual assumption in stellar simulations, the convective boundary is neither spherical nor static. This resolves a paradox of mixing length theory, in which the convective velocity has a discontinuity at the convective boundary, going from a finite value to zero.

The surface of separation is a nonspherical comoving (Lagrangian) boundary, which moves relative to the spherical (Eulerian) boundaries of a stellar evolution code. The spherical shells do move on average with the matter, in that they may contain a fixed amount of mass, but it need not be the same matter. While the interface moves across a spherical shell, it may later move back. Motion does not necessarily give mixing. Note that this goes beyond the usual notion of spherical Lagrangian shells in a stellar evolutionary code; hydrodynamic motion is faster than slow secular evolution, so that the spherical shells seem relatively fixed in space (that is, Eulerian); see Cox (1980).

2.3. g-modes

To the extent that the time scale for heating and cooling the radiative region is longer than that for hydrodynamic motion, Kelvin’s circulation theorem holds (Landau & Lifshitz 1959). Further, if the hydrodynamic motion is slow (strongly subsonic), it is described by a velocity potential, $\mathbf{v} = \nabla\phi$, where ϕ satisfies Laplace’s equation $\nabla^2\phi = 0$. If we take a Cartesian coordinate system (x,y,z) with z positive along the radial direction \mathbf{r} , $z = 0$ at the interface between convection and nonconvection, and assume the waveform transverse to z is periodic, then

$$\phi = f(z)e^{i(k_x x + k_y y - \omega t)}, \quad (4)$$

so

$$\nabla^2\phi = \phi(-(k_x^2 + k_y^2) + \frac{1}{f}\frac{\partial^2 f}{\partial z^2}) = 0, \quad (5)$$

giving $f = e^{\pm kz}$, where k is the transverse wave number, defined by $k^2 = k_x^2 + k_y^2$. The sign choice comes from the boundary condition, so that the function decreases exponentially away from the boundary $z = 0$. Waves of longer wavelength (small k) extend farther from the boundary. While this is a useful guide, the actual waves (AA00) are not strictly incompressible ($\nabla \cdot \mathbf{v} = 0$; density variations occur, and are important for damping the waves).

We relate the wave number to the frequency by equating the acceleration in the z direction to the corresponding force per unit mass. For an incompressible liquid it gives

$\omega^2 = kg$, while the compressible case results in the Brunt-Väisälä frequency

$$N^2 = \frac{g\delta}{H_P}(\nabla_{ad} - \nabla + \frac{\varphi}{\delta}\nabla_{\mu}), \quad (6)$$

from Kippenhahn & Weigert (1990), eq. 6.18, where the symbols have their usual meaning, or Hansen & Kawaler (1994), eq. 5.35 and 10.92. Our system is finite, so only a discrete spectrum of waves is possible. Notice that the quantity in parenthesis is the Ledoux condition for convective instability, and has implications for regions with compositional gradients, which we do not pursue here.

The longest wavelengths penetrate further, and will be most effective for mixing. The maximum wavelength generated will depend upon the details of the convective driving.

With a complete theory of turbulent convection we could simply determine a transfer function for the excitation of waves in the radiative region (Goldreich, Murray, & Kumar 1994). Mixing length theory is the simplest; it maintains that only one dominant wavelength need be considered — the mixing length. The Canuto-Mazzitelli theory gives a broader spectrum of modes but they peak in the same place (see (Canuto & Mazzitelli 1991), Figure 1). For simplicity we take the appropriate wavelength to be equal to the length scale we would derive from the size of the plumes seen in simulations.

2.4. Dissipation of waves

The driving of the waves must be balanced by their dissipation for a steady state to result. In the stellar plasma this will usually be due to thermal diffusion of radiation. Such dissipation will be faster at the shorter wavelengths; for a given amplitude they have the largest gradients. For a given wave, we could integrate the wave equation (Cox 1980) for a precise result. The precision would be illusory in that the range of relevant wavelengths would depend upon our ignorance of the properties of the convective driving. Instead we give a simpler example to illustrate the physics and make a preliminary estimate of the importance of the process.

The canonical picture of damping of gravity waves is by viscosity (Landau & Lifshitz (1959), §25). Using the viscosity of a plasma in the absence of magnetic fields (Spitzer (1962), §5.5), we find a damping time of many gigayears for stellar conditions, so this is not the relevant damping. The compressible effects give rise to temperature fluctuations; this gives a pressure perturbation which resists the wave motion, analogous to damping of stellar pulsations (Cox 1980). Following Kumar & Quataert (1997), the local radiative dissipation

of gravity waves is

$$\gamma \approx \frac{2F_r k_r^2 H_T}{5P}, \quad (7)$$

where F_r is the radiative flux at radius r from the center of the star, $k_r \approx N[l(l+1)]^{\frac{1}{2}}/[r\omega]$ is the wave's radial wave number for frequency ω , P is the pressure, and H_T is the temperature scale height.

2.5. Circulation and mixing

A difficult step is the connection between the multidimensional flow and the microscopic mixing. We argue that dissipation drives circulation, which is likely to be turbulent. For the purposes of a stellar evolution code we identify this with a diffusive velocity $u_k(\Delta r)$, even though the physical identity is not exact. The characteristic scale is l_{turb} , and is determined from simulations.

As we saw above, the coupling of convective plumes with the region of laminar flow outside the convective region generates significant density anisotropies and waves at the boundary. These low Mach number waves can be described approximately as potential flow which we assume to be dissipated over a distance determined by the hydrodynamics. This damping is an entropy-generating process, causing vorticity which allows for microscopic mixing of the material and slow circulation of the mixed material well beyond the convectively neutral boundary. Qualitatively, this is like breaking of wave crests on a sea.

For didactic purposes we will derive the generation of vorticity by damping of the potential flow in a simple plane parallel case. Following Landau & Lifshitz (1959), §9,

$$\frac{d\mathbf{v}}{dt} + \mathbf{v} \cdot \nabla \mathbf{v} = \nabla \mathbf{w} - T \nabla S \quad (8)$$

Discarding $\mathbf{v} \cdot \nabla \mathbf{v}$ as small,

$$\nabla \times \frac{d\mathbf{v}}{dt} = \nabla \times \nabla \mathbf{w} - \nabla \times (T \nabla S) \quad (9)$$

The term $\nabla \times \nabla \mathbf{w} \rightarrow 0$, giving

$$\frac{d\nabla \times \mathbf{v}}{dt} = -T(\nabla \times \nabla S) + \nabla S \times \nabla T \quad (10)$$

Discarding $-T(\nabla \times \nabla S) \rightarrow 0$ gives the final form for the generation of vorticity,

$$\frac{d\nabla \times \mathbf{v}}{dt} = \nabla S \times \nabla T \quad (11)$$

In a perfectly spherically symmetric star $\nabla S \times \nabla T$ would go to zero in the laminar regions. When we introduce perturbations from the damping of the waves, however, we gain a cross

term which makes the time derivative of the vorticity non-zero. We employ a standard style of perturbation analysis *a la* Landau & Lifshitz (1959) or Hansen & Kawaler (1994), discarding terms of higher than first order, and examine the contribution from

$$\frac{d\nabla \times \mathbf{v}}{dt} = \nabla S' \times \nabla T_0 \quad (12)$$

where X' denotes a perturbation and X_0 denotes the unperturbed value of a variable. Henceforth we will change notation to $X = X_0$ for simplicity. In the simplified plane parallel case and ignoring unnecessary constants,

$$\frac{d\nabla \times \mathbf{v}}{dt} = \frac{\partial S'}{\partial x} \times \frac{\partial T}{\partial z} \quad (13)$$

From the standard equations of stellar structure (Kippenhahn & Weigert 1990) we take

$$\frac{\partial T_0}{\partial z} = -\frac{3\kappa\rho L}{16\pi a c r^2 T^3} \hat{z} \quad (14)$$

and from thermodynamics (Reif 1965)

$$\frac{\partial S'}{\partial x} = \frac{1}{T+T'}(4aT^3 \frac{\partial T'}{\partial x} + \frac{P}{\rho^2} \frac{\partial \rho'}{\partial x}) \hat{x} \quad (15)$$

We will assume an adiabatic case, such that $\rho^{\gamma-1}T = \text{const}$ and

$$\frac{\partial \rho'}{\partial x} = \frac{1}{\gamma-1} T'^{\frac{2-\gamma}{\gamma-1}} \frac{\partial T'}{\partial x} \quad (16)$$

After some algebraic manipulation,

$$\begin{aligned} \frac{d\nabla \times \mathbf{v}}{dt} &= \frac{\partial S'}{\partial x} \times \frac{\partial T}{\partial z} = \\ &= -\frac{3\kappa\rho L}{16\pi a c r^2 T^3} \frac{1}{T+T'} (4acT^3 + \frac{1}{\gamma-1} T'^{\frac{2-\gamma}{\gamma-1}} \frac{P}{\rho^2}) \frac{\partial T'}{\partial x} \end{aligned} \quad (17)$$

Integrating over dt with the damping described in §2.4 and a reasonable approximation to the wavefunction gives an estimate of the vorticity. Further using the curl theorem and integrating the vorticity over the path of a fluid element gives an estimate of the diffusion velocity at a given radius.

3. Implementation in stellar evolution

To implement this mixing in TYCHO, we treat the mixing as a diffusion process with a diffusion coefficient

$$D = \frac{u_k(\Delta r)l_{turb}}{3} \quad (18)$$

constructed from the terms discussed in the previous section. This treatment leaves one free parameter, $\frac{l_{turb}}{H_p}$, the dominant scale length of the turbulence near impact of the plumes with the boundary. This quantity is directly related to the dominant wavelength of the gravity waves driving the mixing. There is power at all scales in the convective region. The power is flat or slightly rising from the largest scales to the value we choose for our treatment and then follows a power law consistent with Kolmogorov turbulence down to the smallest resolved scales (Porter et al. 2001). We estimate $\frac{l_{turb}}{H_p} \sim 0.1 - 0.15$ using three-dimensional numerical simulations (Porter et al. 2001). Traditionally, model fits have been improved by introducing free parameters such as the alpha prescription for overshooting (Maeder & Meynet 1989). Clearly, we should not have infinite freedom to introduce parameters. While the parameterized approach has yielded extremely important results in terms of understanding the extent of the extra mixing observed in stars, it gives us little insight into the underlying physics and has limited predictive power. By fixing this quantity using results from multi-dimensional hydro calculations, we are attempting to construct a physical picture of the mixing in the radiative region with minimal variability in parameters. We prefer to constrain our theory by terrestrial simulations and experiment rather than astronomical observation. This should increase the predictive power of the theory. Additional simulations are needed to explore the behavior of this scaling in a wider variety of conditions appropriate to stellar astrophysics. Cases where the pressure scale height is divergent or much larger than the convective scale, for example in the small convective core of the ZAMS sun are of particular interest.

A desirable property falls naturally out of this treatment. Three-dimensional hydro simulations indicate that boundaries with shallow changes in the adiabatic gradient should be able to mix over wider ranges in radii (Brummell, Clune, & Toomre 2002). This should result in more mixing for higher mass stars, and more mixing in convective cores than in envelopes, which seems to be supported by parametrized overshooting in previous work (Pols et al. 1998; Maeder & Meynet 1989). This treatment preserves this behavior, since the region over which the gravity waves are dissipated is larger in the more isentropic environment of core convection. Also, the higher convective velocities in H burning cores than envelopes result in a higher gravity wave flux and larger mixing region, and similarly more mixing in He cores than H. The extra mixing occurs over a significant fraction of a pressure scale height in core convection (compare with values of $0.4-0.6H_p$ in parametrized overshooting) and $\lesssim 0.05-0.1H_p$ for envelope convection.

4. THE STELLAR EVOLUTION CODE TYCHO

All stellar evolution calculations presented below were performed using the TYCHO 1-D stellar evolution code discussed by Young, Mamajek, Arnett, & Liebert (2001) but with substantial improvements in several areas. The equation of state (EOS) has been updated to use a modified version of the Timmes & Swesty (2000) tabular electron-positron EOS. It has been further modified to have appropriate coulomb corrections for the weak screening case and a Debye interpolation for strongly coupled plasmas. This agrees to within 2% (and usually to less than 0.1%) with the EOS tested empirically by the OPAL project’s high energy density laser experiments (Iglesias & Rogers 1996). There are significant deviations from our EOS only where the OPAL models do not account for contributions from electron degeneracy pressure. The size of the reaction network was increased to 175 nuclei, and is well populated all the way up to the iron peak. The low temperature opacities have been completely revised to use tables from Alexander & Ferguson (1994), and are interpolated to serve for any metallicity between zero and five times solar. The mass loss at low T_{eff} has been updated to use the modified Reimers formulation presented in Blöcker (1995), which results in much higher mass loss rates on the AGB. Alternatively, low temperature mass loss may be switched off entirely to examine purely episodic mass loss on the AGB. An ADI operator split has been implemented in the mixing algorithm so that nuclear reaction calculations will be informed about the change in composition, and the thermodynamic variables used in the EOS and mixing routines will properly take into account energy input by burning and neutrino cooling. The mixing is also now time-limited rather than instantaneous. Additional refinements improving the numerical convergence of the code and its convergence at small timesteps have also been incorporated. Experiments have been performed which include heavy element diffusion, and give unsurprising results, consistent with solar models from Bahcall, Pinsonneault, & Basu (2001). The version of the code used in this study (TYCHO 6.11) does not incorporate heavy element diffusion, as such an examination is beyond the scope of the current discussion. It is also useful to separate the effect of settling out from the phenomenon being examined. The timescale for settling is sufficiently long that for ages much less than that of the Sun, the effect should be negligible. The two quantitative cases presented herein both have ages less than 10^9 yr, and should not be affected.

5. COMPARISONS WITH PREVIOUS WORK

Remedies to the problem of mixing have until recently largely been phenomenological. The mixing beyond the standard model is parametrized and labeled as “overshooting” in convective cores and “undershooting” in convective envelopes, or more generically as over-

shooting in both cases. The term has been taken by various groups to encompass both penetrative convection beyond the formal boundary of convective stability and slow compositional mixing. The most common overshooting prescription is “alpha-overshoot”, where compositional mixing is arbitrarily extended some fraction of a pressure scale height beyond the boundary of the formally convective region (Maeder & Meynet 1989). More recently, Pols et al. (1998) have devised a parameterization based upon the superadiabatic excess of the boundary, which has the advantage of being tied to the structure of the star. Parameter fitting of this sort is valuable in constraining the extent of the extra mixing by astronomical observation, but gives us little insight into the physical nature of the process. Overshooting based on rotational mixing has also been proposed. It has been particularly useful in solving the problem of the lithium gap in F stars. The blue side of the dip is reasonably well modelled by rotation-driven meridional circulation (Deliyannis et al. 1998; Boesgaard & King 2002; Piau & Turck-Chièze 2002; Pinsonneault et al. 2002). Recent work describing angular momentum transport by gravity waves has shown considerable success in matching the red side of the dip (Charbonnel & Talon 1999; Talon, Kumar, & Zahn 2002). Rotation looks likely to be an important contributor to the solution of the mixing problem, but is probably not the whole of the story (Maeder & Meynet 1989; Pinsonneault et al. 2002). It is our intention to avoid the use of the term “overshooting” entirely so as to be free of its associated connotations.

In this paper we discuss non-rotational hydrodynamic contributions to the mixing from gravity waves generated at the surface of separation between the convective and laminar regions of a star. García López & Spruit (1991) attempt to assess the contribution to mixing of gravity waves at the convective boundary in the particular context of lithium depletion in F type stars in young clusters. They conclude that the mechanism produces the proper mixing behavior, but requires a gravity wave flux a factor of fifteen larger than given by simple estimates. This problem is not insurmountable. They themselves point out that the efficiency of converting kinetic energy of convective fluid elements increases significantly if the downflows driving the waves are concentrated into narrow plumes. Simulations show the filling factors of these plumes are a few percent (Porter et al. 2001; Brummell, Clune, & Toomre 2002). In addition, Canuto (2002) argues that turbulent mixing in a stellar context is likely to persist for a larger range of conditions. In García López & Spruit (1991), the extent of mixing was limited by comparing an unperturbed stellar model to a laminar stability model. The critical Richardson number $Ri(cr)$ for which turbulence may persist once established is a factor of four larger than $Ri^l(cr)$ for the breakdown of an established laminar flow. In addition, radiative losses weaken stable stratification and the gravity waves themselves act as an energy source for turbulence. Thus $Ri^{tot}(cr)$ may be substantially larger than $Ri^l(cr)$. This allows the spatial extent of turbulence and associated mixing

for a given gravity wave flux to be larger by about the same factor (Canuto 2002). A combination of these effects could easily allow the gravity wave mechanism of García López & Spruit (1991) to account for the mixing in this case. By examining the dissipation from an energetic standpoint and using a length scale calibrated by fully non-linear hydro codes with energy sources and sinks, we hope to avoid this particular difficulty. The García López & Spruit (1991) treatment has certain advantages. Gravity wave spectra may be dominated by frequencies which are weakly damped or resonant with characteristic length scales in the star. We do not initially take this into account. Such a treatment is necessary for treating angular momentum transport by gravity waves (Charbonnel & Talon 1999; Talon, Kumar, & Zahn 2002), and is likely to be important in the non-rotational context as well.

6. TESTS OF THE THEORY

In this section we present comparisons of models produced by the TYCHO code incorporating the new convective boundary conditions with observations in three different evolutionary regimes. This theoretical description provides useful physical insight into envelope convection and light element nucleosynthesis, cluster ages and gross stellar properties including core convection, and complex convection and advanced nucleosynthesis in evolved stars. No parameter optimization was used to improve the fit of any models. Two solar models (one with element diffusion and one without) were also run as a control, and all surface observables (R, T_{eff}, L, X_i) are in acceptable agreement with Bahcall, Pinsonneault, & Basu (2001). Errors in the luminosity and $X(^4He)$ are consistent with the absence of helium and heavy element settling in the non-diffusion version of TYCHO. A detailed comparison with helioseismological constraints on the interior was not performed. However, the model is in qualitative agreement with suggestions that the extent of *penetrative* convection does not extend much beyond that predicted by conventional models, while compositional mixing must go significantly further (Bahcall, Pinsonneault, & Basu 2001). The size of the penetrative convective envelope ($0.727R_\odot$, consistent with the no-diffusion model of Bahcall, Pinsonneault, & Basu (2001) and $0.712R_\odot$, consistent with the diffusion model), is similar in TYCHO models with and without the extra mixing. The slow compositional mixing extends well beyond the standard convective zone ($\sim 5 \times 10^9$ cm) when the new theory is employed.

6.1. Li and Be in the Hyades and Pleiades

The burning of lithium and beryllium in pre-main sequence stars provides a sensitive probe of convective mixing. Lithium is burned at temperatures above 2.5×10^6 K, which

can be reached at the base of convection zones in lower mass stars. A “lithium edge” where the abundance begins to decline from an approximately constant value is produced at low effective temperatures since the depth of convection increases with decreasing stellar mass. The location and steepness of this edge serves to test whether convection in stellar models reaches as deeply as in real stars. A second dip in the lithium abundance is seen in F stars ($T_{eff} \sim 6500 - 7000K$), which requires additional physics, most likely rotation (Thorburn et al. 1993; Charbonnel & Talon 1999; Piau & Turck-Chièze 2002; Boesgaard & King 2002; Pinsonneault et al. 2002; Talon, Kumar, & Zahn 2002) García López & Spruit (1991) present a gravity wave-excited mixing treatment which is somewhat consistent with the observational data for the lithium gap. However, they do not extend the results down to the lithium edge, so a direct comparison with our work is difficult. Recent observations have provided similar data for beryllium, which burns at 3.5×10^6 K and thus provides an additional, related constraint. From a theoretical standpoint, Be depletions are as simple to estimate as those from Li. Unfortunately, the atomic transitions of beryllium are located just below the UV atmospheric cutoff, where ground-based observations of stars with T_{eff} much below 5500 K is difficult. More importantly, at low T_{eff} a line of magnesium begins to come in strongly almost on top of the beryllium line, rendering accurate equivalent width measurements problematic (Thorburn et al. 1993; Piau & Turck-Chièze 2002; Boesgaard & King 2002). The location of the beryllium edge is therefore not known.

Figure 2 (top) shows calculated surface lithium abundances for stars of Hyades composition ($[Fe/H] = +0.13 \pm 0.02$). Values are taken at the age of the best fit isochrone for the cluster determined using photometric data from de Bruijne et al. (2001) and compared with the observed points from Boesgaard & King (2002). The age of the cluster in our models is between 650 and 700 Myr, consistent with the age from conventional overshooting models in de Bruijne et al. (2001). In our simulations, the drop-off in lithium with T_{eff} is much too shallow without the extra slow mixing. Implementing the mixing brings our theoretical values in line with observations. The lithium dip in F stars is not reproduced, which is unsurprising as rotation is not included in these models. We find rather too much depletion of lithium in the models in the range between the F dip and the depletion edge. We suspect this, too, is a hallmark of rotational mixing, as in some regimes mixing appears to actually be *damped* by rotation (Piau & Turck-Chièze 2002; Kippenhahn & Weigert 1990; Chandrasekhar, S. 1961). A full calculation of the wave spectrum should also improve the calculation in this regime. The bottom panel of Figure 2 shows the same data for beryllium. We find no significant depletion. This is consistent with observations to the lowest observed T_{eff} , and indicates that our mixing is not excessive. Interestingly, we do not see any depletion of beryllium at lower effective temperatures. At the age of the Hyades the lowest mass stars have not finished contracting onto the main sequence and have not established

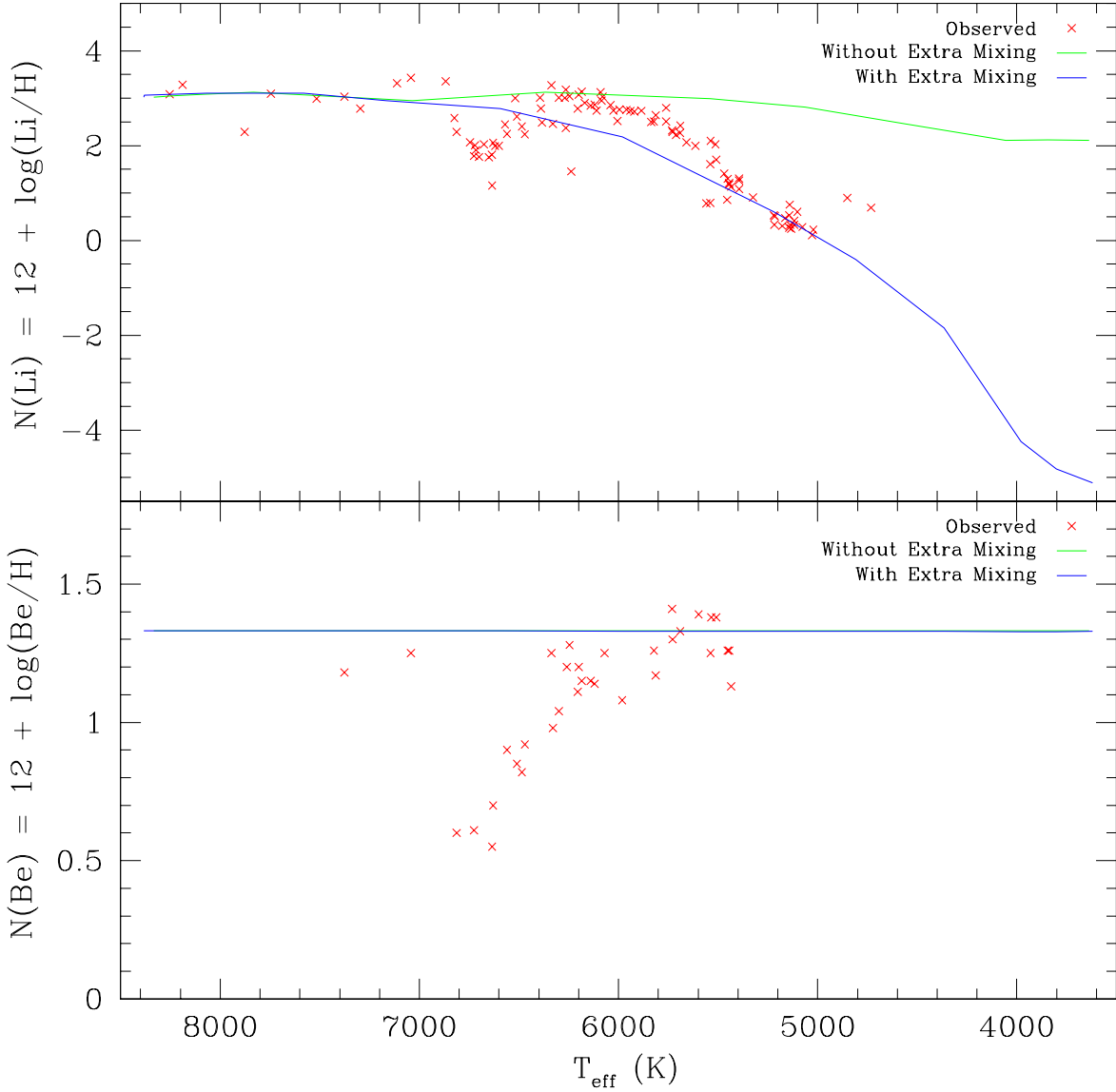


Fig. 2.— Observed Li (top panel) and Be (bottom) abundances from Thorburn et al. (1993); Boesgaard & King (2002) (crosses, red in the electronic version) along with calculated values with extra mixing (solid line, blue in the electronic version) and without (dotted line, green in the electronic version). The model values with slow mixing follow the observed points closely at the depletion edge; those without under-predict the depletion significantly. We suspect that the dips at $T_{eff} \sim 6500 - 7000K$ are due to rotation (Thorburn et al. 1993; Charbonnel & Talon 1999; Piau & Turck-Chièze 2002; Boesgaard & King 2002; Talon, Kumar, & Zahn 2002), indicating that we may be able to separate out the effects of rotation and dissipative hydrodynamic mixing processes. Note that the dips appear at approximately the same effective temperature.

the deep convective envelopes necessary to deplete the beryllium. Space-based observations and data on older clusters could aid in detecting beryllium depletion. The coincidence in effective temperature between the Li and Be dips indicates that this is a sensitive test of the depth of the convective zone. The dip itself may serve as a test of rotation, while the depletion edge tests non-rotational mixing.

Simultaneously being able to reproduce Li depletions for clusters of different ages is problematic for many theories of mixing (Piau & Turck-Chièze 2002). In order to test that our description gives a reasonable time dependence for Li depletion, we modeled the Li edge in the Pleiades. Figure 3 shows the observed points from Soderblom et al. (1993) and models with the additional mixing. Our models were for our best fit turn-off age of 120 Myr (see Section 7.2). The models produce somewhat too much depletion at the lowest T_{eff} , but overall the predicted depletion matches the observations well. The models do not include molecular hydrogen contributions to the EOS, which becomes significant at the masses corresponding to the lowest effective temperatures. More work is required to sort out EOS and opacity effects from the mixing algorithm in this regime.

6.2. Comparison With Li Depletion Ages

The age of the Pleiades has variously been quoted as 75 to 150 Myr, with most studies using a value between 75 – 100 Myr. Recent determinations of the age using the lithium depletion edge in brown dwarfs place the age at 125 Myr (Stauffer et al. 1998). Similar uncertainties exist for other young clusters. Li depletion ages have been determined for two other clusters, α Per and IC 2391, with ages of 90 ± 10 and 53 ± 5 Myr, respectively (Stauffer et al. 1999; Barrado y Navascués, Stauffer, & Patten 1999). Both ages are approximately 50% longer than those derived from conventional main sequence fitting. Without an independent calibration, it is equally possible that the Li depletion ages are wrong and turnoff ages are correct. The depletion ages are, however, consistent with models with parametrized overshooting calibrated by other methods. In the absence of further observational constraints we will take the depletion ages to be a reliable measure. We determine the age of the clusters by fitting the main sequence turnoff with the extra mixing included.

Models were run for masses from 3.0 to 6.0 M_{\odot} in increments of 0.1 M_{\odot} . The models were run at solar metallicity, which is within the error bars for the observations (Boesgaard & Friel 1990; Randich et al. 2001). The L and T_{eff} conversions from observational data are taken from Mamajek (2002). Figure 4 shows our isochrones for the Pleiades (top), α Persei (center), and IC 2391 (bottom) at 120, 75, and 55 Myr, along with observed values corrected for differential reddening across the clusters. The error bars on the observations are sufficiently large that further refinement of the age was not attempted. The turnoff ages with the extra mixing are 120 Myr for the Pleiades, 75 Myr for α Per, and 55 Myr for IC 2391, consistent with the ages determined from lithium depletion in brown dwarfs.

One additional constraint is also reproduced. There is one white dwarf member of the Pleiades with a mass of $\sim 1 M_{\odot}$ (Wegner et al. 1991). Our models produce a white dwarf progenitor of $\sim 1 M_{\odot}$ at the age of the cluster from an initial mass of $\sim 5.5 M_{\odot}$.

6.3. Carbon Stars

The term “carbon star” is variously used to describe a menagerie of objects with surface abundances of carbon enhanced relative to oxygen. The group includes evolved stars on the AGB, subsets of white dwarfs and Wolf-Rayets, and cool dwarfs. Only the first category will be discussed here. The evolved stars further may show enhancements in s-process elements and lithium. Observations of ^{99}Tc , which has a half life of 2×10^5 years, indicates that the products of *in situ* nuclear processing are being mixed to the surface. The s-process elements and enhancements of lithium and ^{13}C require burning in a region enriched in both protons

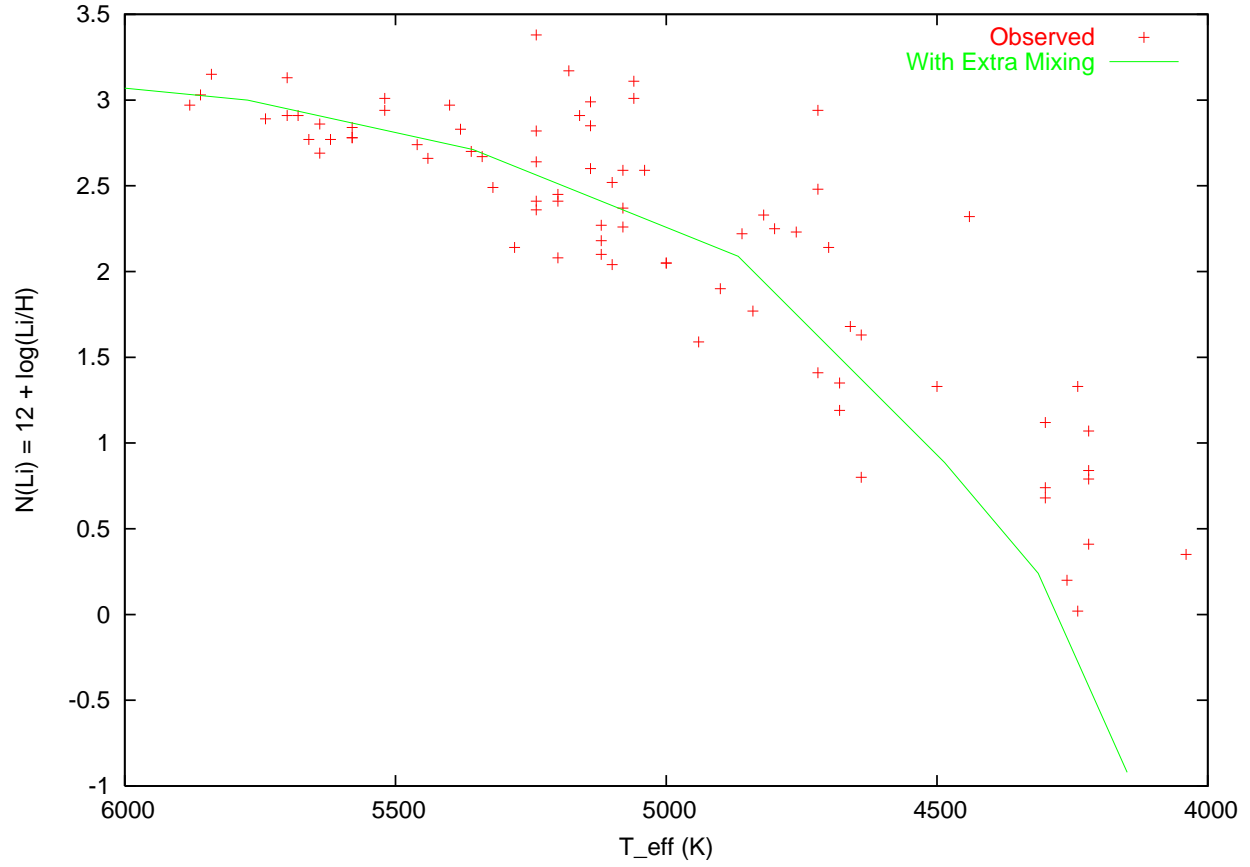


Fig. 3.— Observed Pleiades surface Li abundances (crosses) from Soderblom et al. (1993) plotted with models (solid line) for an age of 120 Myr. The predicted depletions match the observations well except at the lowest T_{eff} . This may be due to an inadequacy in the mixing model or inaccuracies in the low entropy equation of state.

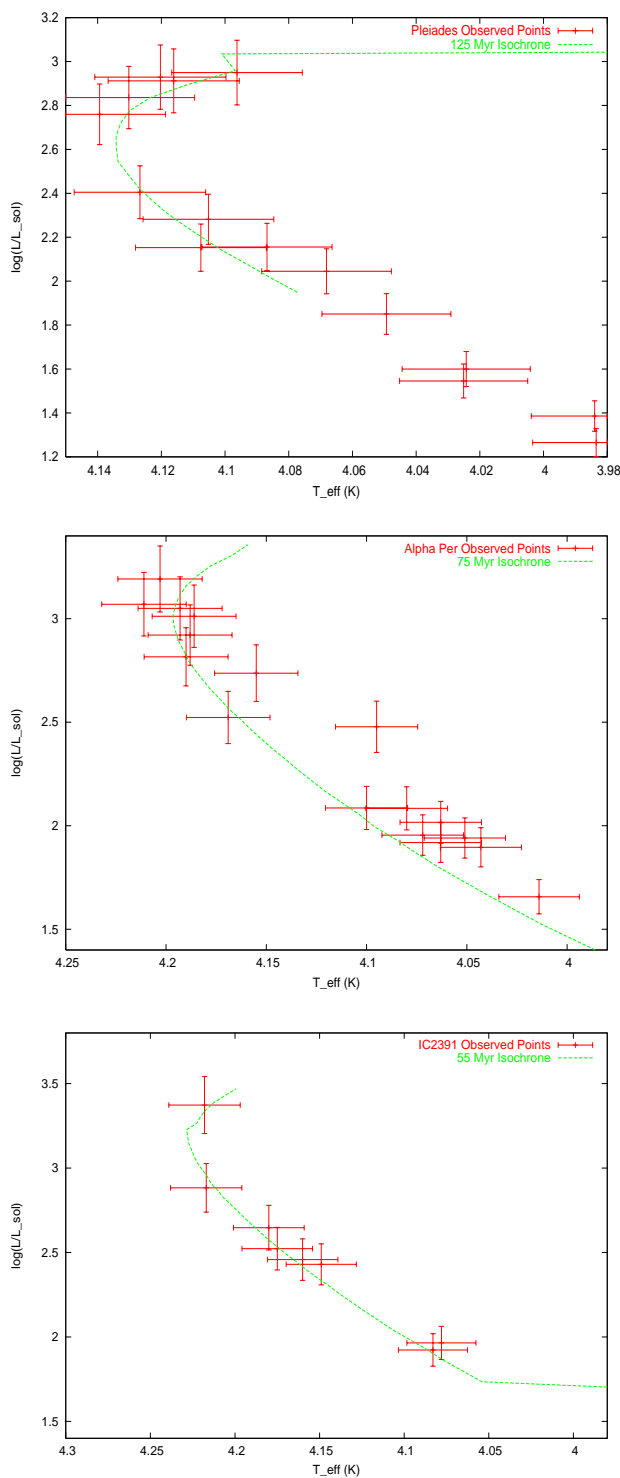


Fig. 4.— Observed luminosity and effective temperature for the turnoff stars of the Pleiades (top), α Persei (center), and IC 2391 (bottom) from Mamajek (2002). Crosses are observed stars and lines represent 120, 75, and 55 Myr isochrones from TYCHO, respectively. The error bars are representative, and do not properly take into account systematic errors. The isochrones are a reasonable fit at the lithium depletion ages of the clusters without recourse to parameter optimization.

and the products of triple α burning (Wallerstein & Knapp 1998; Cameron & Fowler 1971). This is difficult to reproduce with traditional stellar evolution codes, since the products of partial triple α burning are not in general mixed into hydrogen burning regions or further to the surface (Busso et al. 1999).

Making comparisons between models and observed carbon stars is difficult, as the class includes such a large variety of stars. The masses of carbon stars for low metallicity populations appear to range from ~ 0.8 to ~ 6 or $8 M_{\odot}$. Absolute bolometric magnitudes ranging from $M_{\text{bol}} = 0$ to -8 ($L/L_{\odot} \sim 10^2 - 10^5$), $T_{\text{eff}} \sim 2000 - 5000\text{K}$, and radii from approximately 2.4 - 2.7 AU (Wallerstein 1973; Wallerstein & Knapp 1998). Carbon stars appear to come in a range of metallicities, but the ratio of C to M stars increases greatly from the Galactic bulge to the Magellanic Clouds. There is a definite trend toward increasing efficiency of carbon star production at low metallicities (Blanco et al. 1980).

Implementing the present theoretical description of convective boundary conditions in TYCHO, we obtain carbon stars without further modification of the code. In light of the variety inherent in the class, this does not, by itself, demonstrate much about the effectiveness of the treatment, but when considered along with the success in a range of other regimes, is a promising sign. Exact isotope ratios are dependent not only on the boundary conditions, but also on the time dependent treatment of the compositional mixing inside the convective region itself. A subsequent paper will examine CNO and s-process nucleosynthesis for a range of masses and compositions.

We find that a $6 M_{\odot}$ star at $z = 0.001$ produces a star with surface carbon in excess of oxygen at the beginning of the thermal pulse AGB. The luminosity and T_{eff} are consistent with observed quantities for C-N stars. Carbon approaches but never exceeds oxygen for a solar metallicity model, as we might expect from the observed bias toward low metallicity environments. Figure 5 shows the surface abundances of ${}^7\text{Li}$, ${}^{12}\text{C}$, ${}^{13}\text{C}$, ${}^{14}\text{N}$, and ${}^{16}\text{O}$ for the final 10^5 years of the model track. The star shows a pulse of elevated lithium and ${}^{13}\text{C}/{}^{12}\text{C}$ ratio at the beginning of the carbon star phase. This is consistent with the (again, wide range of) observed values for C-N stars, which show a bimodal distribution in carbon isotope ratios and enhanced lithium values. This may reflect an evolutionary trend (Wallerstein & Knapp 1998).

7. CONCLUSIONS

We take a novel approach to the problem of mixing in stars by identifying phenomena which emerge in nonlocal, nonlinear, multi-dimensional hydro simulations. These simulations

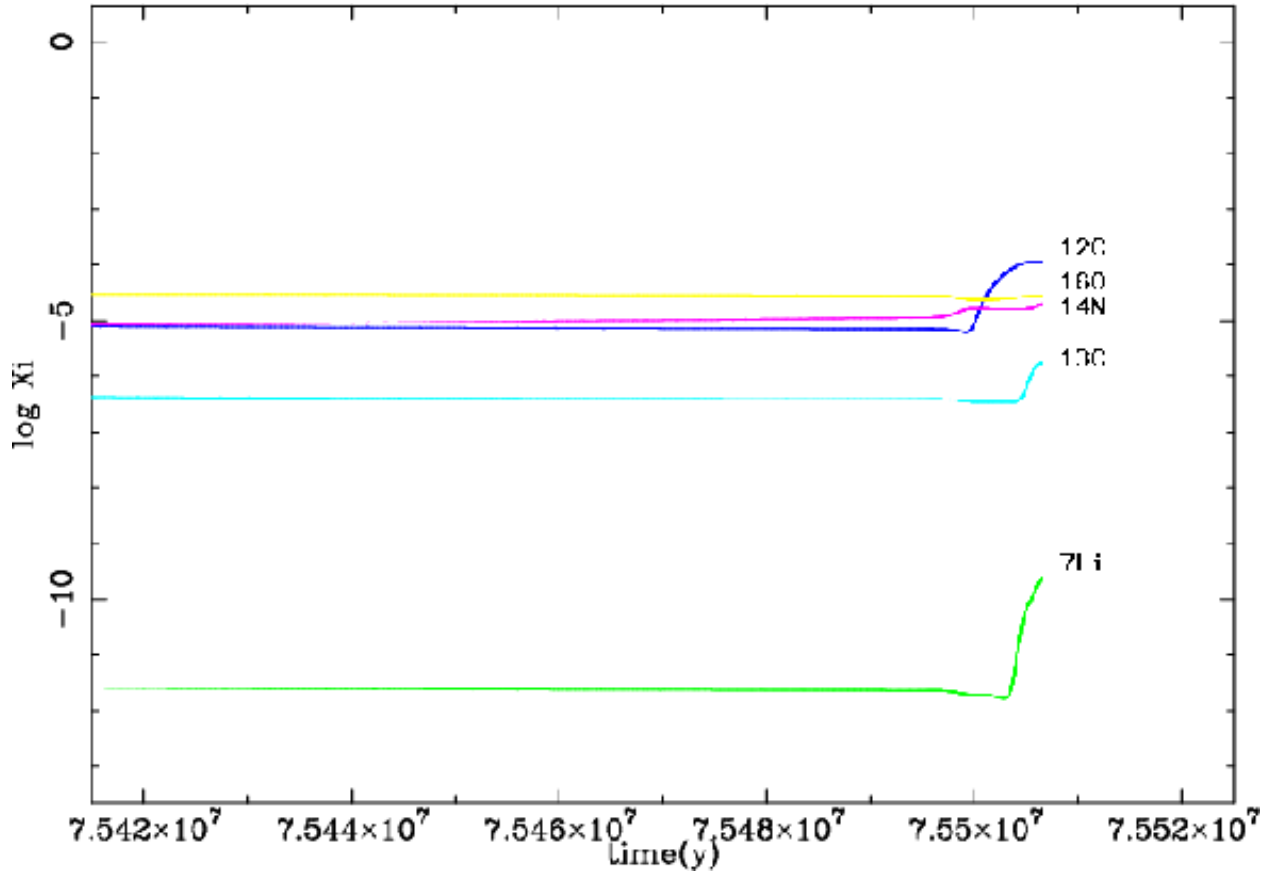


Fig. 5.— Surface abundances of ${}^7\text{Li}$, ${}^{12}\text{C}$, ${}^{13}\text{C}$, ${}^{14}\text{N}$, and ${}^{16}\text{O}$ for the final 10^5 years of a $z = 0.001$ $6 M_{\odot}$ model evolutionary track, corresponding to the beginning of the thermal pulse AGB. The carbon abundance has exceeded oxygen at the surface and is accompanied by a pulse of ${}^7\text{Li}$ and ${}^{13}\text{C}$.

appear to successfully reproduce behavior on the large scale which transport most of the flux of energy and material. We then develop a theoretical description of this large scale behavior. This facilitates the transition from observed phenomenology to a predictive understanding which can be of use in the wider context of stellar evolution.

Several fundamental, if not surprising, results arise from implementing such a physical theory. First, the boundary between convectively stable and unstable regions cannot be treated as spherical or static, even in a one-dimensional approximation of the sort necessary for stellar evolution calculations. Hydrodynamic processes seen in multiple dimensions must be taken into account. Second, a careful treatment of the boundary conditions always results in extra mixing beyond the formal boundary. Third, a single physical process operates in both core and surface convective zones. Fourth, implementation of this theory in the stellar evolution code TYCHO contributes significantly to solving problems in several different regimes of stellar evolution. This is accomplished with only one parameter that does not fall directly out of the theoretical description, namely the dominant wavelength of the gravity waves driving the slow circulation in the radiative zone. Even this parameter is (a) a quantity with physical meaning, and (b) not allowed to vary, being fixed by data from numerical simulations. Finally, if this model continues to be as successful as it has thus far at explaining non-rotationally induced mixing, it will allow us to isolate the rotational contribution to stellar physics with a fair degree of confidence.

We reproduce the Li depletion edge in the Hyades and Pleiades. We find cluster ages for three young clusters consistent with ages determined from measurements of Li in brown dwarfs and for the Hyades as determined by main-sequence fitting with alpha-overshoot. The theory also generates reasonable carbon star models on the AGB. We expect that the physics and nucleosynthetic yields of supernovae and gamma ray bursts may be sensitive to the rotational properties of the star, core sizes, and final composition profiles at core collapse. It is essential to produce accurate initial models in order to generate realistic models of the explosion. This requires a physical, rather than simply phenomenological, characterization of the hydrodynamic mixing and rotation in stars. These factors also influence chemical enrichment from AGB stars and thermonuclear supernovae. These results may significantly improve our understanding of these processes, which impact issues as disparate as cluster ages, and thus timescales observed for disk evolution in pre-Main Sequence stars, to the nucleosynthetic history of the universe.

We stress that this result is merely a first step toward completely and predictively characterizing the mixing in stars. Numerical simulations have already illuminated physical processes which have changed our understanding of stellar astrophysics. Experiments with higher resolution, more complete physics, and a wider variety of geometries and thermody-

dynamic conditions appropriate to the range encountered in stars are vital, as they may well display yet more complex phenomena. Several other processes remain to be integrated into a complete picture of stellar mixing. This treatment does not take into account the effect of magnetic fields, which provide an upwardly biased buoyancy force and, when overlapping the convective boundary, coupling between stable and unstable fluids. Coupling between rotation and convective fluid motions must also be considered. Finally, changes to the nuclear burning and convection resulting from the ingestion of fresh fuel into a convective core or shell must be more carefully explored. We are confident, however, that the careful treatment of stellar hydrodynamics in both convective and radiative regions, plays an essential role in understanding the important problem of mixing in stars.

REFERENCES

- Alexander, D. R. & Ferguson, J. W. 1994, *ApJ*, 437, 879
- Asida, S.M., & Arnett, D. 2000 *ApJ*, 545, 435
- Bahcall, J. N., Pinsonneault, M. H., & Basu, S. 2001, *ApJ*, 555, 990
- Barrado y Navascués, D., Stauffer, J. R., & Patten, B. M. 1999, *ApJ*, 522, L53
- Bazàn, G., & Arnett, D. 1998, *ApJ*, 494, 316
- Blanco, V. M., Blanco, B. M., & McCarthy, M. F. 1980, *ApJ*, 242, 938
- Blöcker, T. 1995, *A&A*, 297, 727
- Boesgaard, A. M. & King, J. R. 2002, *ApJ*, 565, 587
- Boesgaard, A. M. & Friel, E. D. 1990, *ApJ*, 351, 467
- Brummell, N. H., Clune, T. L., & Toomre, J. 2002, *ApJ*, 570, 825
- Busso, M., Gallino, R., & Wasserburg, G. J. 1999, *ARA&A*, 37, 239
- Cameron, A. G. W. & Fowler, W. A. 1971, *ApJ*, 164, 111
- Canuto, V. M. & Mazzitelli, I., 1991, *ApJ*, 370, 295
- Canuto, V. M. 2000, *ApJ*, 571, L79
- Canuto, V. M. 2002, *A&A*, 384, 1119

- Chandrasekhar, S. 1961, *Hydrodynamic and Hydromagnetic Instability*, Oxford University Press, London
- Charbonnel, C., & Talon, S., 1999, A&A, 351, 635
- Christensen-Dalsgaard, J. 2002, Rev Mod Phys, in press
- Clayton, D. D. 1983, *Principles of Stellar Evolution and Nucleosynthesis*, University of Chicago Press, Chicago
- Cowling, T. G., 1941, MNRAS, 101, 367
- Cox, J. P., 1980, *Theory of Stellar Pulsations*, Princeton University Press, Princeton NJ
- de Bruijne, J. H. J., Hoogerwerf, R., & de Zeeuw, P. T. 2001, A&A, 367, 111
- Deliyannis, C. P., Boesgaard, A. M., Stephens, A., King, J. R., & Vogt, S. S. 1998, ApJ, 498, L147
- Dimotakis, P. E. 2001, APS, DPP LM2.004
- Freytag, B., Ludwig, H.-G., & Steffan, M., 1996, —aap, 313, 497
- García López, R. J. & Spruit, H. C. 1991, ApJ, 377, 268
- Golreich, P., N. Murray, & Kumar, P., 1994, ApJ, 424, 466
- Hansen, C. J., & Kawaler, S. D., 1994, *Stellar Interiors*, Springer-Verlag
- Hurlburt, N. E., Toomre, J., & Massaguer, J. M., ApJ, 311, 563
- Iglesias, C. & Rogers, F. J. 1996, ApJ, 464, 943
- Kippenhahn, R. & Weigert, A. 1990, *Stellar Structure and Evolution*, Springer-Verlag
- Kumar, P., & Quataert, E. J., 1997, ApJ, 475, L143
- Landau, L. D. & Lifshitz, E. M. 1959, Fluid Mechanics, Pergamon Press, London
- Maeder, A. & Meynet, G. 1989, A&A, 84, L89
- Mamajek, E. E. 2002, private communication
- Piau, L. & Turck-Chièze, S. 2002, ApJ, 566, 419
- Pinsonneault, M. H., Steigman, G., Walker, T. P., & Narayanan, V. K. 2002, ApJ, 574, 398

- Pols, O. R., Schröder, K-P., Hurley, J. R., Tout, C. A., & Eggleton, P. P., & Han, Z. 1998, MNRAS, 298, 525
- Pols, O. R., Tout, C. A., Schröder, K-P., Eggleton, P. P., & Manners, J. 1997, MNRAS, 289, 869
- Porter, D., Woodward, P., Toomre, J., & Brummel, N. H. 2001, www.lcse.umn.edu/MOVIES
- Randich, S., Pallavicini, R., Meola, G., Stauffer, J. R., & Balachandran, S. C. 2001, A&A, 372, 862
- Reif, F. 1965, *Fundamentals of Statistical and Thermal Physics*, McGraw-Hill Book Co., N.Y.
- Ribas, I., Jordi, C., Torra, J., & Giménez, Á. 2000, MNRAS, 313, 99
- Saslaw, W. C. & Schwarzschild, M., 1965, ApJ, 142, 1468
- Schatzman, E., 1999, Ap&SS, 265, 97
- Shaviv, G. & Salpeter, E. E., 1973, ApJ, 184, 191
- Soderblom, D. R., Jones, B. F., Balachandran, S., Stauffer, J. R., Duncan, D. K., Fedele, S. B., & Hudon, J. D. 1993, ApJ, 106, 1059
- Spiegel, E. 1972, ARA&A, 10, 261
- Spitzer, L., 1962, *Physics of Fully Ionized Gases*, Interscience Publishers, NY
- Stauffer, J. R., Schultz, G., & Kirkpatrick, J. D. 1998, ApJ, 499, L199
- Stauffer, J. R., Barrado y Navascués, D., Bouvier, J., Morrison, H. L., Harding, P., Luhman, K. L., Stanke, T., McCaughrean, M., Terndrup, D. M., Allen, L., & Assouad, P. 1999, ApJ, 527, 219
- Stein, R. F. 1967, Sol. Phys., 2, 385
- Talon, S., Kumar, P., & Zahn, J-P., 2002, ApJ, 574, L175
- Thorburn, J. A., Hobbs, L. M., Deliyannis, C. P., & Pinsonneault, M. H. 1993, ApJ, 415, 150
- Timmes, F. X. & Swesty, F. D. 2000, ApJS, 126, 501
- Wallerstein, G. 1973, ARA&A, 11, 115

Wallerstein, G., & Knapp, G. R. 1998, *ARA&A*, 36, 369

Wegner, G., Reid, I. N., & McMahan, R. K. Jr. 1991, *ApJ*, 376, 186

Young, P. A., Mamajek, E. E., Arnett, D., & Liebert, J. 2001, *ApJ*, 556, 230